The University Of Sheffield.

This is a repository copy of *Effective estimation of the desired-signal subspace and its application to robust adaptive beamforming*.

White Rose Research Online URL for this paper:
http://eprints.whiterose.ac.uk/120208/

Version: Accepted Version

White Rose
university consortium
Universities of Leeds, Sheffield & York

eprints@whiterose.ac.uk
https://eprints.whiterose.ac.uk/

EFFECTIVE ESTIMATION OF THE DESIRED-SIGNAL SUBSPACE AND ITS APPLICATION TO ROBUST ADAPTIVE BEAMFORMING

Zhenyu Zhang[1], Wen Leng[1], Anguo Wang[1], Wei Liu[2], and Heping Shi[3]

[1] School of Electronic Information Engineering
Tianjin University, Tianjin, P.R. China.
[2]Department of Electronic and Electrical Engineering
University of Sheffield, Sheffield, S1 3JD, United Kingdom
[3]School of Automotion and Transportation
Tianjin University of Technology and Education, Tianjin, P.R. China

ABSTRACT

An effective method is proposed to estimate the desired-signal (S) subspace by the intersection between the signal-plus-interference (SI) subspace and a reference space covering the angular region where the desired signal is located. The estimated S subspace is robust to steering vector mismatch and overestimation of the SI subspace, capable of detecting the relative strength of the desired signal. And even the basis of the estimated S subspace can serve as an effective estimation of the steering vector of the desired signal. With these properties, the estimated S subspace can help to select a more accurate narrow area for searching for the steering vector of the desired signal in mismatch cases. The proposed method is applied for robust adaptive beamforming with an improved performance, as demonstrated by simulation results.

Index Terms— Eigenspace, intersection, robust adaptive beamforming (RAB), steering vector estimation.

1. INTRODUCTION

Adaptive beamforming is one of the most important research areas in array signal processing and has found many applications such as wireless communications, radar, sonar, speech processing, medical imaging, and radio astronomy [1–3]. Among the various state-of-the-art beamformers, the minimum variance distortionless response (MVDR) based beamformer [4] has received tremendous attention, and many MVDR-based robust beamformers were developed to improve their performance under array manifold errors and steering vector mismatches [5–7].

Based on the analytical solution to the traditional MVDR optimization problem, there are mainly two approaches for improving the robustness of the system. One approach is to estimate the interference-plus-noise matrix using prior knowledge such as array calibration and the angular sector where the desired signal is located [8, 9]. The other one is to estimate the steering vector of the desired signal, with the eigenspace-based beamformer being a representative example, applicable to the arbitrary steering vector mismatch case [10]. However, one issue with the eigenspace-based

beamformer is subspace swap in low-SNR scenarios. An enhanced eigenspace-based beamformer named vector space projection (VSP) beamformer was proposed to combat pointing error by estimating the steering vector as well as the power of signal of interest (SOI), by assuming the number of interferences is known [13]. However, the VSP method cannot realize the intended intersection effectively and therefore only gives a very rough estimation of the steering vector of SOI. Another two examples for the latter approach are the optimization-based beamformers proposed in [11, 12]: one is called sequential-quadratic-programming-based (SQP) beamformer and the other one is called least-prior-knowledge-based (LP) beamformer. They adopt an orthogonal projector onto a reference space, which is supposed to distinguish the angular region of the desired signal, to limit the search of the desired steering vector around the SOI. In detail, the SQP beamformer aims to estimate the steering vector of SOI directly from the reference space by correcting the presumed steering vector with its orthogonal component, while by relaxing the strict limitation that the estimated steering vector of SOI belongs to the reference space, the LP beamformer gets more degrees of freedom (DOFs) and outperforms the SQP beamformer. Compared with the eigenspace-based beamformer, the SQP/LP beamformer relies on the reference space to have a rough separation between the SOI and the interferences. On the other hand, the eigenspace-based beamformer tries to extract the whole signal plus interference (SI) subspace instead of separating them.

In this work, we combine the approaches of both the SQP/LP beamformer and the eigenspace-based beamfomer and propose an intersection method to achieve a more accurate estimation of the desired-signal (S) subspace, so that the robustness of the beamformer can be enhanced. The key idea of this paper is to realise that the S subspace must lies in both the reference space discussed in [11, 12], and the SI subspace used in the eigenspace-based beamformer. the basis of the estimated S subspace by considering the intersection of both spaces can serve as an effective estimation of the desired steering vector. This newly estimated S subspace is robust to steering vector mismatch and overestimation of the SI subspace, capable of detecting the relative strength of the SOI. Modified versions of the SQP beamformer, the LP beamformer, and the MVDR beamformer are obtained by adopting the newly estimated S subspace, as shown by simulation results, all of them have achieved an improved performance compared to the original versions.

This paper is structured as follows. Some background of MVDR-based beamforming is presented in Section 2. The theorems and properties of the estimated S subspace is discussed in Section 3. In Section 4, simulation results are provided to show the properties of the estimated S subspace and the performance improvements of several existing beamformers modified by the estimated S subspace. Conclusions are drawn in Section 5.

2. BACKGROUND

Consider a narrowband linear array of M sensors. The $M \times 1$ complex observation vector at time k can be modeled as $\mathbf{x}(k) = \mathbf{s}(k) + \mathbf{i}(k) + \mathbf{n}(k)$, where $\mathbf{s}(k) = s(k)\mathbf{a}$, $\mathbf{i}(k)$ and $\mathbf{n}(k)$ are the statistically uncorrelated components of the desired signal, interference and noise, respectively, $s(k)$ is the desired signal waveform, and $\mathbf{a}$ is its steering vector.

Applying the complex weight vector $\mathbf{w} = [w_1, ..., w_M]^T \in \mathbb{C}^M$ to $\mathbf{x}(k)$, we obtain the beamformer output $y(k) = \mathbf{w}^H \mathbf{x}(k)$. The beamformer output signal-to-interference-plus-noise ratio (SINR) is defined as

$$\text{SINR} = \frac{\sigma_s^2 |\mathbf{w}^H \mathbf{a}|^2}{\mathbf{w}^H \mathbf{R}_{i+n} \mathbf{w}}, \qquad (1)$$

where σ_s^2 is the power of desired signal, $\mathbf{R}_{i+n}$ is the interference plus noise covariance (INC) matrix. Minimizing the output interference-plus-noise power subject to a distortionless response toward the desired signal leads to the following optimization problem

$$\min_{\mathbf{w}} \quad \mathbf{w}^H \mathbf{R}_{i+n} \mathbf{w} \quad \text{subject to} \quad \mathbf{w}^H \mathbf{a} = 1, \qquad (2)$$

the solution is given by:

$$\mathbf{w}_{opt} = \frac{\mathbf{R}_{i+n}^{-1} \mathbf{a}}{\mathbf{a}^H \mathbf{R}_{i+n}^{-1} \mathbf{a}}. \qquad (3)$$

We can replace $\mathbf{R}_{i+n}$ by the covariance matrix $\mathbf{R}$ of $\mathbf{x}(k)$, which leads to the classic MVDR beamformer, with the same optimum solution. In practice, the exact INC matrix $\mathbf{R}_{i+n}$ (or $\mathbf{R}$) and the actual steering vector $\mathbf{a}$ are unavailable. Therefore, the sample covariance matrix $\mathbf{R}_x = \frac{1}{K} \sum_{k=1}^{K} \mathbf{x}(k)\mathbf{x}^H(k)$ and the presumed steering vector $\mathbf{a}_p$ are used instead. Here, K is the number of data snapshots. In this case, equation (3) changes to

$$\mathbf{w}_x = \frac{\mathbf{R}_x^{-1} \mathbf{a}_p}{\mathbf{a}_p^H \mathbf{R}_x^{-1} \mathbf{a}_p}, \qquad (4)$$

which is often referred to as the MVDR-SMI (sample matrix inversion) beamformer.

3. DESIRED-SIGNAL (S) SUBSPACE ESTIMATION

As we know, the SI subspace is spanned by the steering vectors of the SOI and the interferences. Given a reference space which contains the steering vectors for an angular sector where only the SOI is located, the intersection between the SI subspace and such a reference space will generally result to a more accurate estimation of the S subspace, which is spanned by the steering vector of SOI only. Employing the orthogonal projector onto the S subspace, we can obtain a new criterion for determining how close a steering vector is located to the steering vector of SOI. This will contribute to the choice of the feasible region in all kinds of optimization problems for modifying the presumed steering vector.

In practice, for the traditional eigenspace-based beamformer, we estimate the SI subspace by K_R dominant eigenvectors of $\mathbf{R}_x$. The value of K_R can be found as follows: let $\{s_i\}_{i=1}^{M}$ denote the set of eigenvalues of $\mathbf{R}_x$, sorted in descending order; then K_R is chosen as the i which maximizes s_{i-1}/s_i, with i starting from 2. To estimate the required reference space, the method used in [11, 12] is adopted: let $\mathbf{C} = \int_{\Theta} \mathbf{d}(\theta) \mathbf{d}^H(\theta) d\theta$ ($\mathbf{d}(\theta)$ is the steering vector of direction θ and it relates to the sensor array geometry); then the K_C dominant eigenvectors of $\mathbf{C}$ are selected to span the reference space. K_C is only related to the array geometry and can be set in advance if the array geometry is known. For example, for an angular sector with $10°$ width (around the broadside), $K_C = 3$ is tested to be a good choice in a 10-sensor half-wavelength-spaced uniform linear array (ULA).

The estimated SI subspace and the estimated reference space are denoted by $\mathbf{\Omega}_R$ and $\mathbf{\Omega}_C$, respectively. Let $\mathbf{\Omega}_R = \text{span}\{\mathbf{B}\}$ and $\mathbf{\Omega}_C = \text{span}\{\mathbf{D}\}$, where $\mathbf{B}$ and $\mathbf{D}$ are a collection of orthogonal bases of $\mathbf{\Omega}_R$ and $\mathbf{\Omega}_C$, respectively. Although it is relatively easy to obtain $\mathbf{\Omega}_C$ and $\mathbf{\Omega}_R$ through the two matrices $\mathbf{C}$ and $\mathbf{R}_x$, there is no clear path for obtaining the intersection $\mathbf{\Omega}_C \cap \mathbf{\Omega}_R$ of the two matrices [14,15], not to mention the orthogonal projection onto $\mathbf{\Omega}_C \cap \mathbf{\Omega}_R$.

In the following, by analyzing the inter-projection $\mathbf{D}\mathbf{D}^H \mathbf{B}\mathbf{B}^H$, we provide an approximate solution to the problem of obtaining the orthogonal projector onto the space $\mathbf{\Omega}_C \cap \mathbf{\Omega}_R$. First, considering the following theorem:

Theorem 1: $\mathbf{B}\mathbf{B}^H \lim_{n \to \infty} \mathbf{P}^n \mathbf{x}$ ($\mathbf{P} = \mathbf{D}\mathbf{D}^H \mathbf{B}\mathbf{B}^H$) approximates the orthogonal projector onto $\mathbf{\Omega}_C \cap \mathbf{\Omega}_R$.

Proof: Assume $\mathbf{\Omega}_C = \text{span}\{\mathbf{D}\} \subset \mathbf{\Omega}$ and $\mathbf{\Omega}_R = \text{span}\{\mathbf{B}\} \subset \mathbf{\Omega}$. For $\forall \mathbf{x} \in \mathbf{\Omega}$, $\mathbf{x}$ can be orthogonally decomposed into

$$\mathbf{x} = \mathbf{x}_\parallel + \mathbf{x}_\perp, \qquad (5)$$

where $\mathbf{x}_\parallel \in \mathbf{\Omega}_C \cap \mathbf{\Omega}_R$ and $\mathbf{x}_\perp \perp \mathbf{\Omega}_C \cap \mathbf{\Omega}_R$. Let $\mathbf{P} = \mathbf{D}\mathbf{D}^H \mathbf{B}\mathbf{B}^H$, then,

$$\mathbf{P}\mathbf{x}_\parallel = \mathbf{x}_\parallel. \qquad (6)$$

$\mathbf{P}\mathbf{x}_\perp$ is the orthogonal projection of $\mathbf{B}\mathbf{B}^H \mathbf{x}_\perp$ onto $\mathbf{\Omega}_C$ and $\mathbf{B}\mathbf{B}^H \mathbf{x}_\perp$ is the orthogonal projection of $\mathbf{x}_\perp$ onto $\mathbf{\Omega}_R$. So $\exists d_1, d_2$ $(d_1, d_2 \geq 0)$, $\|\mathbf{P}\mathbf{x}_\perp\|^2 + d_1^2 = \|\mathbf{B}\mathbf{B}^H \mathbf{x}_\perp\|^2$ and $\|\mathbf{B}\mathbf{B}^H \mathbf{x}_\perp\|^2 + d_2^2 = \|\mathbf{x}_\perp\|^2$, that is $\|\mathbf{P}\mathbf{x}_\perp\|^2 + d_1^2 + d_2^2 = \|\mathbf{x}_\perp\|^2$. Therefore

$$\|\mathbf{P}\mathbf{x}_\perp\| \leq \|\mathbf{x}_\perp\|. \qquad (7)$$

Note the equality holds only when $\mathbf{x}_\perp$ is a zero vector.

Additionally, since $\mathbf{x}_\perp \perp \mathbf{\Omega}_C \cap \mathbf{\Omega}_R$, $\forall \boldsymbol{\varsigma} \in \mathbf{\Omega}_C \cap \mathbf{\Omega}_R$,

$$(\mathbf{P}\mathbf{x}_\perp)^H \boldsymbol{\varsigma} = \mathbf{x}_\perp{}^H \mathbf{P}^H \boldsymbol{\varsigma} = \mathbf{x}_\perp{}^H \boldsymbol{\varsigma} = 0, \qquad (8)$$

we have $\mathbf{P}\mathbf{x}_\perp \perp \mathbf{\Omega}_C \cap \mathbf{\Omega}_R$, and so does $\mathbf{P}^n \mathbf{x}_\perp \perp \mathbf{\Omega}_C \cap \mathbf{\Omega}_R$ (n is a non-negative integer). According to (7), suppose $\mathbf{x}_\perp$ is not zero, we obtain
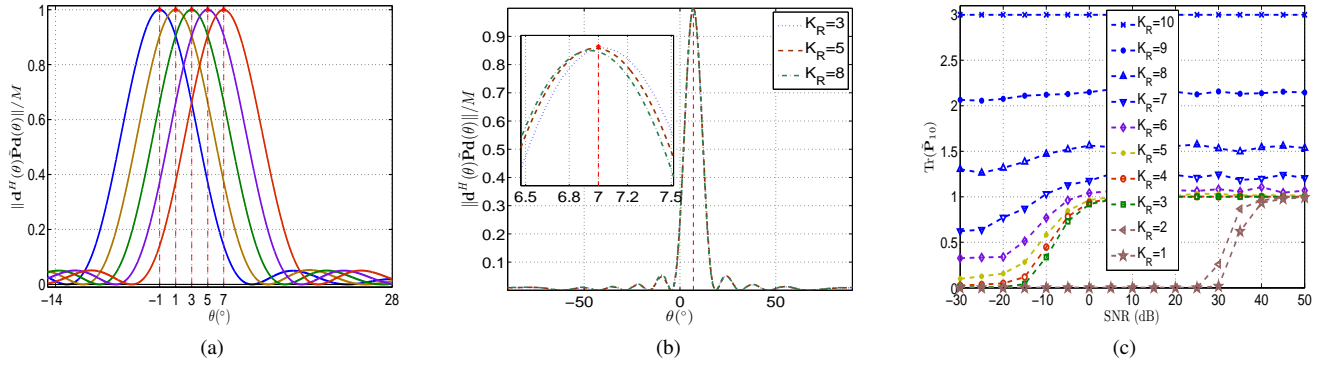
$$\|\mathbf{P}^n \mathbf{x}_\perp\| < \cdots < \|\mathbf{P}\mathbf{x}_\perp\| < \|\mathbf{x}_\perp\|. \qquad (9)$$

There must exist a positive set $\varepsilon_i < 1$, $i = 2, \ldots, n$ to satisfy

$$\|\mathbf{P}^i \mathbf{x}_\perp\| = \varepsilon_{i-1} \|\mathbf{P}^{i-1} \mathbf{x}_\perp\|. \qquad (10)$$

While $\|\mathbf{P}^n \mathbf{x}_\perp\| = \|\mathbf{P}\mathbf{x}_\perp\| \varepsilon_1 \cdot \varepsilon_2 \cdot \cdots \cdot \varepsilon_{n-1} < \|\mathbf{P}\mathbf{x}_\perp\| \cdot \max^n\{\varepsilon_i\} \to 0$, $n \to \infty$, we obtain

$$\lim_{n \to \infty} \mathbf{P}^n \mathbf{x} = \lim_{n \to \infty} \mathbf{P}^n \mathbf{x}_\parallel + 0 = \mathbf{x}_\parallel. \qquad (11)$$

Fig. 1. Simulation I: (a) the norm of $\mathbf{d}^H(\theta)\tilde{\mathbf{P}}\mathbf{d}(\theta)$ versus θ under different θ_s; (b) the norm of $\mathbf{d}^H(\theta)\tilde{\mathbf{P}}\mathbf{d}(\theta)$ versus θ with different K_R; (c) $\mathrm{Tr}(\tilde{\mathbf{P}}_{10})$ versus SNR with different K_R.

Therefore, for $\forall \mathbf{x} \in \mathbf{\Omega}$, $\lim_{n\to\infty} \mathbf{P}^n\mathbf{x}$ will remain the part of $\mathbf{x}$ in $\mathbf{\Omega}_C \cap \mathbf{\Omega}_R$, and exclude the part orthogonal to $\mathbf{\Omega}_C \cap \mathbf{\Omega}_R$, so does $\mathbf{BB}^H \lim_{n\to\infty} \mathbf{P}^n\mathbf{x}$. Denote $\mathbf{BB}^H\mathbf{P}^n$ as $\tilde{\mathbf{P}}_n$. It is clear that $\tilde{\mathbf{P}}_\infty$ is Hermitian. And in the limit of infinity, $\tilde{\mathbf{P}}_\infty^2 = \tilde{\mathbf{P}}_\infty$. In conclusion, $\tilde{\mathbf{P}}_\infty$ is the orthogonal projector onto $\mathbf{\Omega}_C \cap \mathbf{\Omega}_R$.

This completes the proof.

In practice, it is impossible to calculate $\tilde{\mathbf{P}}_\infty$ and we have to consider a finite number of inter-projections. Since the S subspace is one-dimensional, we use the eigenvector corresponding to the largest eigenvalue of $\tilde{\mathbf{P}}_n$ ($n < \infty$), $\mathbf{p}$, to span the estimated S subspace, and the orthogonal projector onto the estimated S subspace is $\tilde{\mathbf{P}} = \mathbf{pp}^H$ instead of $\tilde{\mathbf{P}}_\infty$. Note that $\sqrt{M}\mathbf{p}/\|\mathbf{p}\|$ can serve as a rough estimation of the steering vector of SOI. In our simulations, $\tilde{\mathbf{P}}_{10}$ is used for a good enough approximation.

There are three properties for the estimated S subspace.

Property 1: robustness to steering vector mismatch, i.e. ability to track the SOI.

$\forall \mathbf{d} \in \mathbf{\Omega}$, the projection $\tilde{\mathbf{P}}\mathbf{d}$ only contains the part of $\mathbf{d}$ which is in $\mathbf{\Omega}_C \cap \mathbf{\Omega}_R$. So the norm of the projection $\|\tilde{\mathbf{P}}\mathbf{d}\|$ gets larger when more part of $\mathbf{d}$ is included in the S subspace, which takes place when $\mathbf{d}$ gets closer to the steering vector of SOI. In particular, when only look direction mismatch error exists, the value of $\|\tilde{\mathbf{P}}\mathbf{d}(\theta)\|$ will provide a measurement about how close a given θ is to θ_s.

Property 2: providing a measurement of the strength of SOI.

Due to the subspace swap problem, estimation of the SI subspace $\mathbf{\Omega}_R$ may not be accurate when the SOI is weak. In this case, the steering vector of SOI will not be in $\mathbf{\Omega}_R$, and $\mathbf{\Omega}_C \cap \mathbf{\Omega}_R$ will be a null in theory. According to this, a threshold value can be set for $\mathrm{Tr}(\tilde{\mathbf{P}}_n)$ ($n < \infty$) to determine whether the steering vector of SOI is in $\mathbf{\Omega}_C \cap \mathbf{\Omega}_R$ or not, which implies whether the SOI is strong enough or not. There are some robust adaptive beamforming (RAB) techniques especially suitable for low signal-to-noise ratio (SNR) or high SNR cases. So this property can serve as a trigger to switch between RAB techniques for low-SNR case and those for high SNR case.

Property 3: robustness to overestimated SI subspace.

When K_R is overestimated, the information of noise subspace will be included in the estimated SI subspace $\mathbf{\Omega}_R$. However, the noise subspace has much less overlap with the reference space (no overlap at all in theory) than that of the real SI subspace with the reference space. So the operation $\mathbf{\Omega}_C \cap \mathbf{\Omega}_R$ will effectively remove the overestimated noise subspace and still result to a good estimation of the S subspace.
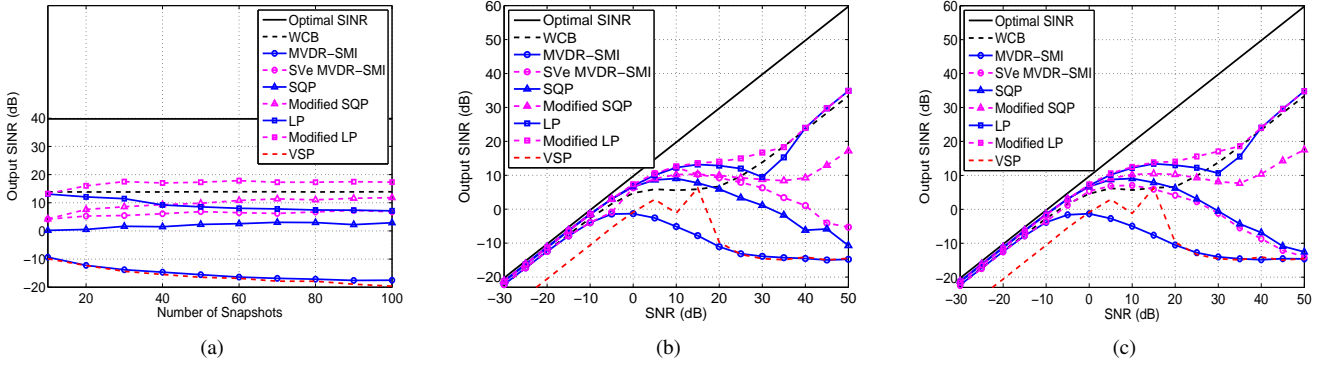
4. SIMULATION RESULTS

In all simulations, a ULA of 10 omnidirectional sensors with half wavelength inter-element spacing is employed. Additive noise at the sensors is modeled as spatially and temporally white complex Gaussian noise with zero mean and unit variance. Two interfering signals arrive from the directions $30°$ and $50°$, respectively, both with an interference-to-noise ratio (INR) of 30dB at each sensor. The presumed DOA angle of SOI is $\theta_p = 3°$ unless otherwise specified. Θ is set to be $[\theta_p - 5°, \theta_p + 5°]$. In the proposed estimation of the S subspace, K_R is chosen adaptively, unless otherwise specified, as described in the second paragraph of Section II, $K_C = 3$ is set in advance and the projector $\tilde{\mathbf{P}}$ is obtained by the dominant eigenvectors of $\tilde{\mathbf{P}}_{10}$. Two sets of simulations are provided. In the first set, the three properties of the estimated S subspace by the proposed method are verified; in the second set, the estimated S subspace is applied to existing robust beamforming methods to show the improved performance in the presence of signal-look-direction mismatch errors and sensor position errors.

4.1. Simulation 1: Demonstrate the Three Properties

The number of data samples $K = 30$, SNR is 20dB, and θ_s is set at $-1°$, $1°$, $3°$, $5°$, and $7°$, respectively. Fig. 1a shows the norm of $\mathbf{d}^H(\theta)\tilde{\mathbf{P}}\mathbf{d}(\theta)$ versus θ under different θ_s. It can be seen that with different levels of SOI-look-direction mismatch, the norm of $\mathbf{d}^H(\theta)\tilde{\mathbf{P}}\mathbf{d}(\theta)$ always reaches its maximum value around the actual DOA, tracking the SOI direction successfully.

Now we set $\theta_s = 7°$, and K_R to be 3, 5, 8, respectively. Fig. 1b shows the norm of $\mathbf{d}^H(\theta)\tilde{\mathbf{P}}\mathbf{d}(\theta)$ versus θ under different K_R. As shown, even when K_R is overestimated, the norm of $\mathbf{d}^H(\theta)\tilde{\mathbf{P}}\mathbf{d}(\theta)$ almost remains the same, again demonstrating the robustness of the estimated S subspace for an overestimated K_R.

Then, K_R is changed from 1 to 10 and Fig. 1c shows the value of $\mathrm{Tr}(\tilde{\mathbf{P}}_{10})$ versus the input SNR with different K_R. As can be

Fig. 2. Simulation II: (a) output SINR versus the number of snapshots K for fixed SNR=30dB; (b) output SINR versus SNR for the number of snapshots K=30 and adaptively chosen K_R; (c) output SINR versus SNR for number of snapshots K=30 and an overestimated $K_R = 6$.

seen, when $K_R = 1, 2$, which means the estimated $\mathbf{\Omega}_R$ misses one or two incoming signals, $\text{Tr}(\tilde{\mathbf{P}}_{10})$ turns large when the SNR is over 30dB, i.e. the SOI is stronger than the interferences. When $K_R = 3, 4, 5, 6$, which means the $\mathbf{\Omega}_R$ contains all the incoming signals and may be overestimated, there is a clear ramp from 0 to 1 between SNR=-20dB and SNR=0dB. If a threshold is set at 0.5, the possible SOI with SNR more than -10dB can be identified for all K_R from 3 to 6, which is consistent with Property 2, and together with the result in Fig. 1b, we can see its robustness to an overestimated K_R. For $K_R = 7, 8, 9, 10$, $\mathbf{\Omega}_R$ is overestimated too much and it becomes very difficult to estimate the power level of SOI from $\text{Tr}(\tilde{\mathbf{P}}_{10})$.

4.2. Simulation 2: Improved Performance for Existing Steering-Vector-Estimation-Based Beamformers

In this part, the SQP beamformer [11], the LP beamformer [12], and the MVDR-SMI beamformer in (4) are modified by employing the proposed estimation of the S subspace as follows: when $\text{Tr}(\tilde{\mathbf{P}}_{10})$ is over 0.5, the first constraint in the optimization problem of SQP beamformer (equation (15) in [11]) is replaced by $\left\|(\mathbf{I} - \tilde{\mathbf{P}})(\mathbf{a}_p + \mathbf{e})\right\| < \sqrt{0.3}$ (where $\mathbf{a}_p$ corresponds to the $\mathbf{p}$ in [11]; and the edge value 0.3 is a rough choice to bound the feasible area, the same below) to obtain the modified SQP beamformer; the second constraints in the optimization problem of LP beamformer (equation (39) in [12]) is replaced by $\text{Tr}((\mathbf{I} - \tilde{\mathbf{P}})\mathbf{A}) < 0.3$ to obtain the modified LP beamformer; and $\mathbf{a}_p$ is replaced by $\sqrt{M}\mathbf{p}/\|\mathbf{p}\|$ in (4) to obtain the steering-vector-estimation-based (SVe) MVDR-SMI beamformer. The worst-case-based (WCB) beamformer in [16] with $\epsilon = 0.3M$ and the VSP beamformer in [13] with expected pointing errors of $4°$ are also simulated for comparison. The relaxing value as defined in the original paper [11] is set as $\delta = 0.1$ and $K_C = 3$ dominant eigenvectors of $\mathbf{C}$ are used for the SQP beamformer. In simulations, the direction mismatch error is assumed to be randomly and uniformly distributed in $[-4°, 4°]$ for both the SOI and the interferences, each sensor is assumed to be randomly displaced from the original location and the displacement is drawn uniformly from the set $[-0.05, 0.05]$ measured in wavelength. For obtaining each point in the curves, 500 independent runs are performed. Here the random DOAs and sensor locations change from run to run but remain fixed from snapshot to snapshot.

In Fig. 2a, the mean output SINRs for the WCB beamformer, the original and modified versions of the SQP beamformer, the LP beamformer and the MVDR beamformer are provided versus the number of training snapshots for fixed SNR=30dB, with Fig. 2b showing the mean output SINRs of the same methods versus the input SNR for fixed data size $K = 30$. It is clear that SNR=-10dB serves as a boundary: on its left, the modified beamformers have the same performance as their corresponding original versions; on its right, the modified beamformers outperforms their counterparts in terms of output SINR. This boundary shows the effectiveness of Property 2 and the improvement in performance is mainly due to the proposed narrower but more accurate feasible region (Property 1) which is focused on the SOI and thus prevents the estimated steering vector converging to a less effective local optimal solution.

To further demonstrate its robustness to an overestimated SI subspace, in the next simulation, we choose a large $K_R = 6$. Fig. 2c gives the mean output SINR of all the aforementioned beamformers versus the input SNR for a fixed data size $K = 30$. Compared with Fig. 2b, in the new figure, except for the SVe MVDR-SMI beamformer (whose performance has degraded but still comparable to the SQP beamformer), the other modified beamformers maintain roughly the same performance with the overestimated K_R. The decline in the performance of SVe MVDR-SMI beamformer is due to distortion in the estimated S subspace caused by the overestimated K_R, as shown in Fig. 1b. The distortion is small but the MVDR-based beamformer is sensitive to it, especially when SNR is large.

5. CONCLUSION

An intersection method has been proposed for more effective estimation of the S subspace. The new estimation is robust to steering vector mismatch and overestimation of the SI subspace, capable of detecting the relative strength of the desired signal. With these properties, the estimated S subspace can be used to reduce the steering vector mismatch error of the desired signal, which in turn leads to improved beamforming performance for several representative RAB methods, as verified by simulation results.

6. REFERENCES

[1] H. L. Van Trees, *Detection, Estimation, and Modulation, Part IV: Theory Optimum Array Processing*. New York: Wiley, 2002.

[2] W. Liu and S. Weiss, *Wideband Beamforming: Concepts and Techniques*. Chichester, UK: John Wiley & Sons, 2010.

[3] J. Li and P. Stocia, *Robust Adaptive Beamforming*. New York: Wiley, 2005.

[4] J. Capon. "High-resolution frequency-wavenumber spectrum analysis," *Proc. IEEE*, vol. 57, pp. 1408–1418, 1969.

[5] R. G. Lorenz and S. P. Boyd, "Robust minimum variance beamforming," in IEEE Transactions on Signal Processing, vol. 53, no. 5, pp. 1684-1696, May 2005.

[6] S. A. Vorobyov, "Principles of minimum variance robust adaptive beamforming design," *Signal Process.*, vol. 93, pp. 3264–3277, Dec. 2013.

[7] L. Zhang and W. Liu, "Robust forward backward based beamformer for a general-rank signal model with real-valued implementation," *Signal Process.*, vol. 92, pp. 163–169, January 2012.

[8] Y. Gu and A. Leshem, "Robust adaptive beamforming based on interference covariance matrix reconstruction and steering vector estimation," *IEEE Trans. Signal Process.*, vol. 60, pp. 3881–3885, Jul. 2012.

[9] Z. Zhang, W. Liu, W. Leng, A. Wang and H. Shi, "Interference-plus-Noise covariance matrix reconstruction via spatial power spectrum sampling for robust adaptive beamforming," *IEEE Signal Process. Lett.*, vol. 23, pp. 121–125, Jan. 2016.

[10] L. Chang and C. C. Yeh,"Performance of DMI and eigenspace-based beamformers," *IEEE Transactions on Antennas and Propagation*, vol. 40, pp. 1336–1347, 1992.

[11] A. Hassanien, S. A. Vorobyov, and K. M. Wong, "Robust adaptive beamforming using sequential quadratic programming: An iterative solution to the mismatch problem," *IEEE Signal Process. Lett.*, vol. 15, pp. 733–736, 2008.

[12] A. Khabbazibasmenj, S. A. Vorobyov, and A. Hassanien, "Robust adaptive beamforming based on steering vector estimation with as little as possible prior information," *IEEE Trans. Signal Process.*, vol. 60, pp. 2974–2987, Jun. 2012.

[13] J. Zhuang and A. Manikas, "Interference cancellation beamforming robust to pointing errors," in IET Signal Processing, vol. 7, no. 2, pp. 120-127, April 2013.

[14] C. R. Rao and S. K. Mitra, "Generalized inverse of matrices and its applications," Calcutta, India: John Wiley & Sons, 1971.

[15] R. A. Horn and C. R. Johnson, "Matrix analysis," Baltimore: Cambridge University Press, 1990.

[16] S. A. Vorobyov, A. B. Gershman, and Z. Q. Luo, "Robust adaptive beamforming using worst-case performance optimization: A solution to the signal mismatch problem," *IEEE Trans. Signal Process.*, vol. 51, pp. 313–324, Feb. 2003.